

NJC

Accepted Manuscript



This is an *Accepted Manuscript*, which has been through the Royal Society of Chemistry peer review process and has been accepted for publication.

Accepted Manuscripts are published online shortly after acceptance, before technical editing, formatting and proof reading. Using this free service, authors can make their results available to the community, in citable form, before we publish the edited article. We will replace this *Accepted Manuscript* with the edited and formatted *Advance Article* as soon as it is available.

You can find more information about *Accepted Manuscripts* in the [Information for Authors](#).

Please note that technical editing may introduce minor changes to the text and/or graphics, which may alter content. The journal's standard [Terms & Conditions](#) and the [Ethical guidelines](#) still apply. In no event shall the Royal Society of Chemistry be held responsible for any errors or omissions in this *Accepted Manuscript* or any consequences arising from the use of any information it contains.



www.rsc.org/njc

Triazole appended BODIPY-piperazine conjugates and their efficacy toward mercury sensing

Roop Shikha Singh, Rakesh Kumar Gupta, Rajendra Prasad Paitandi, Arvind Misra, and Daya Shankar Pandey*

Department of Chemistry, Faculty of Science, Banaras Hindu University, Varanasi - 221 005 (U.P.) India

Abstract

An expeditious synthesis of new click based BODIPY-piperazine conjugates separated by alkyl spacers (**4–7**) has been described. The compounds under investigation have been thoroughly characterized by various physicochemical techniques *viz.*, elemental analyses, IR, HRMS, NMR (^1H , ^{13}C , ^{11}B and ^{19}F), electronic absorption, emission and theoretical studies. Comparative sensing ability of **4–7** toward a range of metal ions has been investigated by various methods. Amongst these compounds only **7** exhibited appreciable selectivity towards Hg^{2+} , while other remain silent in presence of various metal ions. Binding constant and Job's plot analysis indicated 1:1 stoichiometry between **7** and Hg^{2+} . HRMS data and theoretical studies undoubtedly indicated formation of **7**· Hg^{2+} complex and interaction of Hg^{2+} with the probe through nitrogen atom from the piperazine and triazole units.

* To whom correspondence should be addressed. E mail: dspbhu@bhu.ac.in. Phone + 91 542 6702480; FAX + 91 542 2368174

Introduction

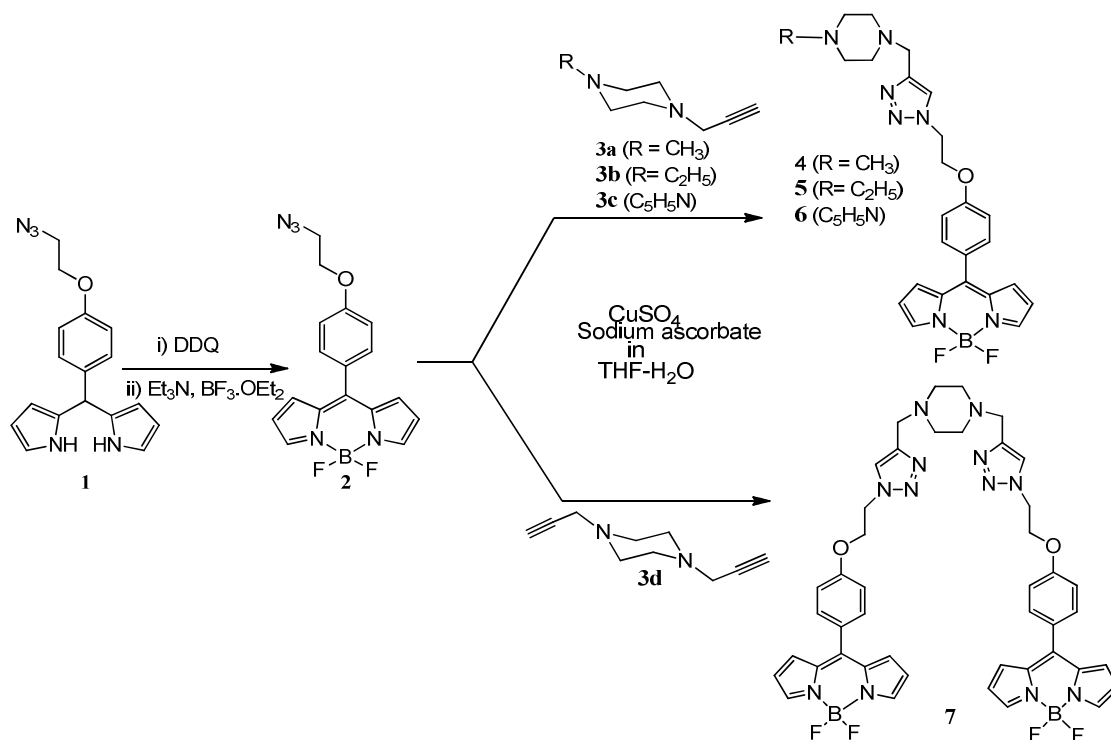
Contemporary chemical research has seen a large surge toward development of novel systems for detection of heavy and transition metal ions (HTMs) because of their association with the environmental and health issues.¹ Among these, Hg^{2+} in its various forms is known as a detrimental neurological toxin which is continuously being introduced in the environment by various natural processes, industrial releases, and anthropogenic activities.² Its bio-accumulation in the living tissues of human and animal bodies *via* food chain causes mercury poisoning, serious neural disorder, and other diseases.^{1,2} Numerous reports dealing with detection of Hg^{2+} are based on fluorescence quenching, because Hg^{2+} induces spin-orbit coupling³ and is spectroscopically and magnetically silent (filled d^{10} orbitals). Therefore, common analytical techniques like nuclear magnetic resonance (NMR) and electron paramagnetic resonance (EPR) are not adequately proficient for detection of Hg^{2+} in the environment and biological systems. In this context, efforts have been made toward development of various optochemical sensors employing diverse chemical transducers and optical principles.⁴ Moreover, development of naked-eye chemosensors for detection of HTMs have drawn special attention, since “naked-eye” detection can offer desired qualitative and quantitative information. In this regard, chemosensors based on rhodamine⁵, fluorescein⁵, naphthalimide⁵, porphyrin⁵ and 4,4-difluoro-4-bora-3a,4a-diaza-s-indacene (BODIPY) etc. have drawn attention of many research groups. Among these, BODIPYs are preferred in the development of fluorescent sensors due to their robustness against light and chemicals, high extinction coefficients, excellent quantum yield, and good solubility. Moreover, spectroscopic and photophysical properties of BODIPYs can be fine tuned by modifying dipyrin core.⁶

Additionally, Cu(I)-catalyzed click reactions between terminal alkynes and azides have been extremely popular in creating molecular diversity. These simple transformations lead to highly regioselective 1,4-di-substituted triazoles in excellent yield and are beneficial in construction of the ligands with cation-chelating ability.⁷ Moreover, substituted piperazine-based ligands have been demanding since these adopt various conformations and can control geometry of the metal complexes.^{8,16} With an objective of developing selective and sensitive fluorescent sensors containing a fluorophore and metal recognition unit i.e, fluoroionophore a series of triazole appended BODIPY-piperazine conjugates **4**, **5**, **6** and **7** have been successfully synthesized. Possibility of the metal recognition has been explored by varying fluoroionophores from un-

substituted to N-substituted piperazine and triazole units employing single (**4–6**) to double click (**7**) reactions. The fluorophore–spacer–chelator construct working on the principle of photo-induced electron transfer (PET) based fluorescence quenching enables **7** to serve as a selective fluoro- and chromogenic probe for Hg^{2+} . Through this contribution we present a small library of BODIPY-piperazine conjugates **4**, **5**, **6** and **7**. Also, we describe herein their comparative sensing ability toward various metal ions. The studies advocated that **7** exhibits significant chromo- and fluorogenic response toward Hg^{2+} .

Results and discussion

As shown in scheme 1, azido BODIPY **2** has been synthesized following literature procedures.⁹ Piperazine derivatives reacted with propargyl bromide in presence of K_2CO_3 to afford terminal alkynes **3a–d** in good yield. Finally, single click reaction between the azido BODIPY **2** and **3a–c** in presence of CuSO_4 and sodium ascorbate afforded **4**, **5**, and **6** while a double click between **3d** and **2** gave **7** in reasonably good yield.⁹ The synthetic pathway adopted for **4–7** is summarized in Scheme 1.



Scheme 1 Synthesis of **2–7**

The ensuing products have been purified by flash silica gel column chromatography to afford bright orange coloured compounds in good yield. All these have been thoroughly characterized by IR, ^1H , ^{13}C , ^{11}B , ^{19}F NMR and HRMS spectral studies. Triazolyl protons (H_h) in ^1H NMR spectra of the respective compounds resonated at $\sim \delta 7.7$ ppm (7.78, **4**; 7.78, **5**; 7.75, **6**; 7.70, **7**) while those associated with piperazine (H_{jk} , $\text{H}_{jk'}$) appeared between $\delta 2.6$ – 3.6 ppm (2.89, **4**; 2.90, **5**; 2.67 and 3.57, **6**; 2.60, **7**). Notably, piperazine protons for **7** resonated as a broad singlet while those for **4**–**6** emerged as splitted signals. It may be attributed to relatively high symmetry of **7** due to presence of the triazolyl rings at either end of piperazine, while **4**–**6** involve piperazine nitrogen with diverse substituents. It is noteworthy to mention that **6** showed two different signals for piperazine protons, signals due to $\text{H}_{kk'}$ protons appeared at $\delta 3.57$ ppm and those for $\text{H}_{jj'}$ resonated at $\delta 2.67$ ppm. Three different types of methylene protons affirmed occurrence of the click reaction wherein H_f (2H) resonated at $\sim \delta 4.8$ ppm (4.82, **4**; 4.83, **5**; 4.81, **6**; 4.79, **7**) while H_g protons (2H) appeared at $\sim \delta 3.8$ (3.82, **4**; 3.82, **5**; 3.76, **6**; 3.71, **7**) ppm. Similarly, methylene protons (H_i) resonated at $\sim \delta 4.4$ (4.47, **4**; 4.48, **5**; 4.47, **6**; 4.45, **7**) and pyrrole ring protons (6H) at $\sim \delta 6.5$, 6.9 and 7.9 ppm. In the NMR spectrum of **6** signal due to pyridyl ring protons appeared at $\delta 6.68$ and 8.17 ppm. Moreover, ^{11}B and ^{19}F NMR spectra of **4**–**7** showed typical triplet (^{11}B) and quartet (^{19}F) due to B-F coupling (Figs. S1-S9, ESI †).¹⁰

Simulated and observed isotopic mass distribution patterns for **4**–**7** [molecular ion peak $[\text{M} + \text{H}]^+$ at [492.2495 (Obs) 492.2492 (calcd), **4**; 506.2657 (Obs) 506.2649 (calcd), **5**; 555.2601 (Obs) 555.2602 (calcd), **6**; 869.3757 (Obs) 869.3757 (calcd), **7**] (Figs. S10–S13, ESI †) and fragmented peaks are in excellent agreement with respective formulations.

Photophysical properties of **4**–**7** have been investigated by electronic absorption and emission spectral studies ($\text{CH}_3\text{CN}:\text{H}_2\text{O}$; 3:2, v/v). The electronic absorption spectra of **4**–**7** displayed common spectral features with high (386, **4**; 385, **5**; 386, **6**; 350 nm, **7**) and low (494, **4**; 495, **5**; 496, **6**; 493 nm, **7**) energy bands along with a shoulder at ~ 473 nm (Fig. 1). The position and intensity of bands at ~ 495 nm signify $\pi \rightarrow \pi^*$ transitions, recurrently present in analogous systems.¹¹ Likewise, **4**–**7** exhibited typical emission bands due to BODIPY $\pi \rightarrow \pi^*$ transitions at 516, 515, 513 and 521 nm upon excitation at 494, (SS, 22 nm), 495 (SS, 20 nm), 496 (SS, 17 nm) and 493 nm (SS, 28 nm), respectively (Fig. 1; Table S1, ESI †).¹¹

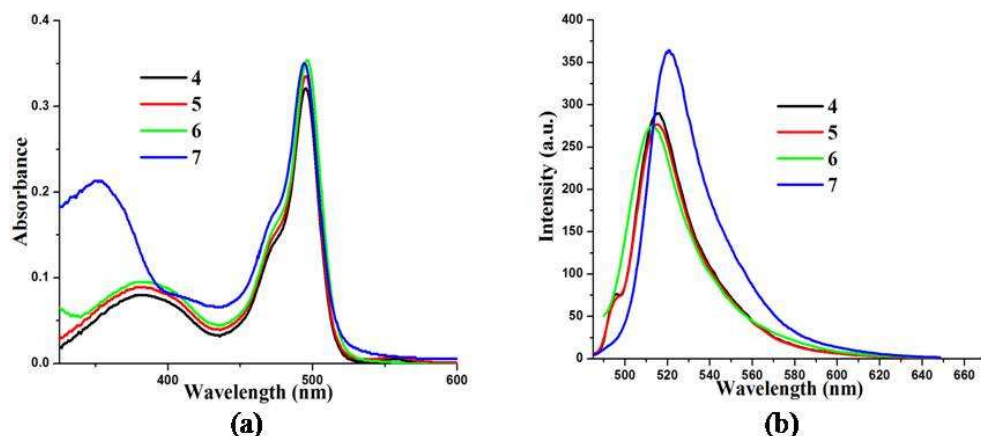


Fig. 1 Absorption (a) and emission (b) spectra of **4–7** (10 μM) in $\text{CH}_3\text{CN}/\text{H}_2\text{O}$ (3 : 2, v/v) .

The compounds under study give coloured solution and are expected to show distinctive colour change upon interaction with various metal ions which may form the basis for naked eye detection. To affirm this, interaction of **4–7** (10 μM) with various metal ions viz., Na^+ , K^+ , Ag^+ , Mg^{2+} , Ca^{2+} , Ni^{2+} , Zn^{2+} , Cd^{2+} , Cu^{2+} , Pb^{2+} , Hg^{2+} , Al^{3+} , Fe^{3+} , and Cr^{3+} [1 mM; $\text{CH}_3\text{CN}/\text{H}_2\text{O}$; (3:2, v/v).] has been investigated. Interestingly, among these, only **7** displayed instantaneous photophysical response toward Hg^{2+} with visible colour change from pale yellow to orange red (Fig. 2). This colorimetric response toward Hg^{2+} persisted for longer durations and we conclude that **7** can act as a potential chromogenic sensor selectively for Hg^{2+} .

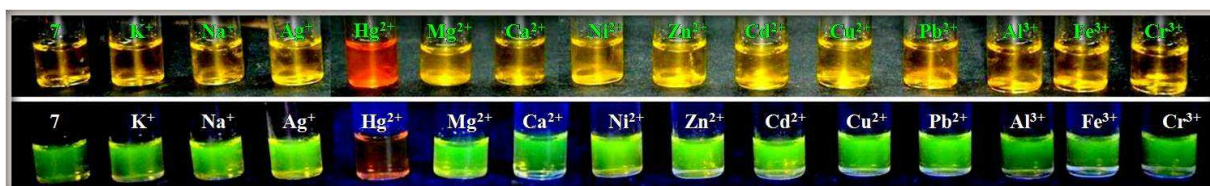


Fig. 2 Top: chromogenic response of **7** ($c = 100 \mu\text{M}$) toward tested metal ions (10 equiv.) Bottom: fluorogenic response of **7** ($c = 100 \mu\text{M}$) for tested metal ions (10 equiv.) under UV light ($\lambda_{\text{ex.}}$ 365 nm).

The electronic absorption spectra of **4–6** do not show any appreciable changes in the position of bands (Fig. S17, ESI †), however, **7** showed considerable shift upon addition of Hg^{2+} . The absorption spectra of **7** upon successive additions of Hg^{2+} (1–10 equiv) displayed decrease and increase in intensity of the bands at 493, and 472 nm, respectively (Fig. 3) along with appearance of a new band at ~ 548 nm. Presumably strong interaction between triazole-piperazine receptor

and Hg^{2+} enhances π delocalization, in turn, reduces energy of the π - π^* transitions.¹² This causes a new noticeable absorption band at ~ 548 nm and changes the colour of solution from pale yellow to orange red. Here we believe that distinctive color changes may arise due to formation of $7\cdot\text{Hg}^{2+}$ complex which has further been supported by HRMS studies (Figs. S14–S15, ESI[†]).

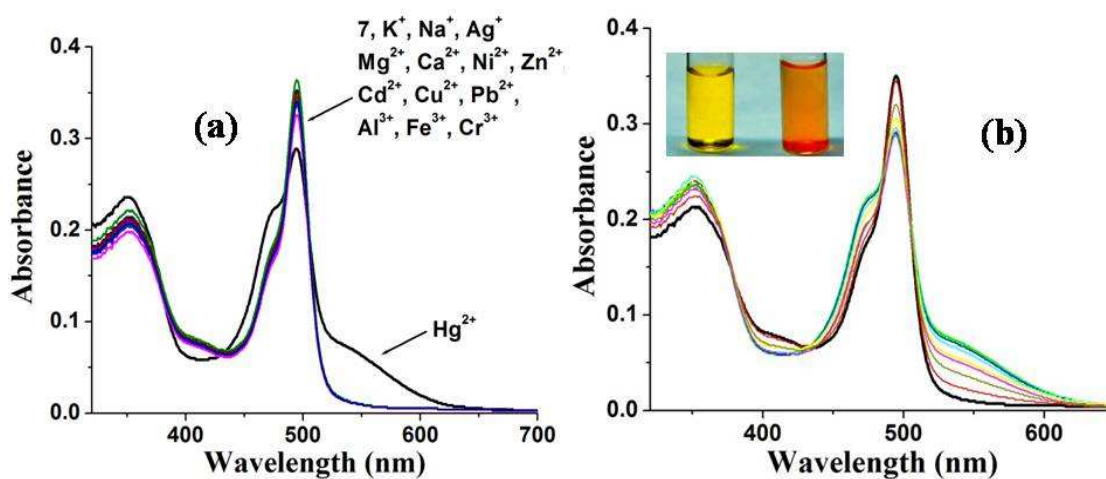


Fig. 3 (a) Absorption spectra of **7** (10 μM) in presence of 10 equiv of various metal ions in $\text{CH}_3\text{CN}/\text{H}_2\text{O}$ (3:2, v/v) (b) the changes in absorption spectrum of **7** (10 μM) in $\text{CH}_3\text{CN}/\text{H}_2\text{O}$ (3:2, v/v) upon addition of Hg^{2+} (1–10 equiv).

In an analogous manner, addition of Hg^{2+} to a solution of **4–7** did not show any alteration in the position and intensity of emission maxima except for **7**, which displayed significant decrease in intensity of the band at 521 nm (Fig. 4). The results suggested that **7** may serve as a selective fluorescent sensor for Hg^{2+} . Further, gradual addition of the Hg^{2+} (1.0–10.0 equiv.) to a solution of **7** led to a decrease in relative fluorescence intensity by ~ 10 and quantum yield by ~ 9 fold (**7**, Φ_{fl} , 28%; $7\cdot\text{Hg}^{2+}$, Φ_{fl} , 3%). The fluorescence quenching thus observed may be attributed to binding of the Hg^{2+} with electron donating piperazine and triazolyl nitrogen and formation of a new species $7\cdot\text{Hg}^{2+}$.¹³

Moreover, interference studies performed by addition of tested metal ions to a solution of $7\cdot\text{Hg}^{2+}$ did not show any significant change in its emission pattern (Fig. S19a, ESI[†]). Stoichiometry between the probe **7** and Hg^{2+} have been deduced from Job's plot analysis by plotting $\chi\cdot\Delta I$ vs molar fraction of **7** keeping total concentration constant. Maximum emission intensity has been obtained at 0.5 molar fractions. The fluorescence changes substantiated 1:1 binding between **7** and Hg^{2+} (Fig. S18a, ESI[†]). The 1:1 binding constant for $7\cdot\text{Hg}^{2+}$ has been

estimated by plotting $1/I - I_0$ vs. $1/Hg^{2+}$ by B-H (Benesi-Hildebrand method) method. The K_a value came out to be $5.2 \times 10^4 \text{ M}^{-1}$ for $7 \cdot Hg^{2+}$ (Fig. 4 inset). The detection limit for Hg^{2+} has been determined by plotting fluorescence intensity vs concentration of the Hg^{2+} which emerged to be $20 \mu\text{M}$, and permits **7** to detect micromolar levels of Hg^{2+} (Fig. S19b, ESI[†]).

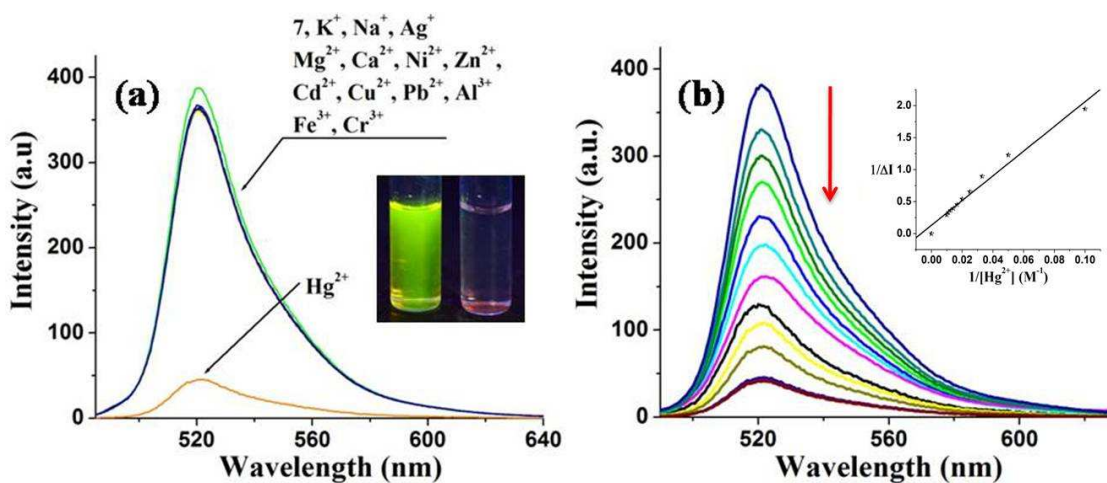


Fig. 4 (a) Fluorescence spectra of **7** ($10 \mu\text{M}$) in presence of 10 equiv of various metal ions in $\text{CH}_3\text{CN}/\text{H}_2\text{O}$ (3:2, v/v) (b) the changes in the fluorescence spectrum of **7** ($10 \mu\text{M}$) in $\text{CH}_3\text{CN}/\text{H}_2\text{O}$ (3:2, v/v) with varying amounts of Hg^{2+} (1–10 equiv) ($\lambda_{\text{ex}} = 493 \text{ nm}$). Inset showing B-H plot for $7 \cdot \text{Hg}^{2+}$.

Aqueous solution of metal nitrates can alter the pH and consequently, photophysical properties of the probe. To ensure that the observed photophysical changes arise exclusively due to presence of Hg^{2+} and not because of change in pH of the probe, pH titration studies using $10 \mu\text{M}$ solution of **7** in $\text{CH}_3\text{CN}/\text{H}_2\text{O}$ (3:2, v/v) have been performed. The pH of probe **7** was varied from 2–12 by adding 10^{-1} M solution of HCl and NaOH with concomitant monitoring of the absorbance and emission intensity. It displayed insignificant change in these properties within the aforesaid pH range (Fig. S20–21, ESI[†]) suggesting insensitivity of the probe toward pH variations.

Reversibility in recognition offers an ideal platform for development of metal sensors as it improves their applicability. Considering the strong binding ability of EDTA towards Hg^{2+} the reversibility of probe **7** has been examined by addition of EDTA. Addition of a large excess of EDTA (50 equiv) to a solution of $7 \cdot \text{Hg}^{2+}$ (**7** + 10 equiv Hg^{2+}) in $\text{CH}_3\text{CN}/\text{H}_2\text{O}$ (3:2, v/v) resulted in restoration of absorption band at 493 and 472 nm along with disappearance of the band at 548

nm. Simultaneously ~ 88 % restoration in emission intensity of band at 521 nm was observed. (Fig. S22, ESI[†]). These results established the probe **7** as a reversible sensor for Hg²⁺ and also eliminated the possibility of it being a chemodosimeter.

Being a heavy metal ion, Hg²⁺ can alter position of the proton signals close to the binding sites.^{14a} To explicitly explore the complexation of **7** with Hg²⁺, ¹H NMR titration studies have been performed. In a typical experiment ¹H NMR spectra of **7** has been acquired in CD₃CN by gradually increasing amount of Hg²⁺ (Fig. 5). Proton corresponding to the triazolyl ring resonated at δ 7.83 ppm, which upon addition of 0.3 equiv of Hg²⁺ shifted downfield to appear at δ 7.90 ppm ($\Delta\delta$, 0.07) as a merged signal with pyrrolic proton. At the same time, methylene protons (H_f, δ 4.74; H_g, δ 3.66; H_i, δ 4.46 ppm) too downfield shifted (H_f, δ 4.76; H_g, δ 3.90; H_i, δ 4.47 ppm). With an increase in the concentration of Hg²⁺ (0.6 equiv) triazolyl proton signal started differentiating from pyrrolic proton along with an additional downfield shift in the position of methylene protons. A total addition of 0.9 equiv of Hg²⁺ resulted in an appreciable downfield shift for triazolyl proton to appear at δ 8.28 ppm ($\Delta\delta$, 0.46) and methylene proton at H_f, δ 4.87 ppm and H_g, δ 4.49 ppm.

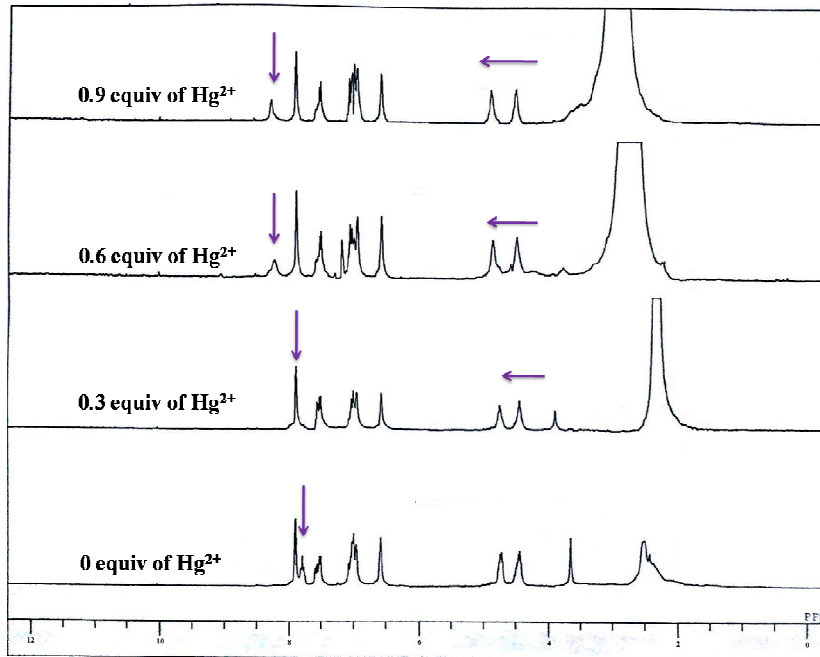


Fig. 5 ¹H NMR spectrum of **7** in CD₃CN with increasing amounts of Hg²⁺ showing formation of **7**·Hg²⁺.

The shift in H_i proton signals could not be monitored at higher concentration of Hg^{2+} (0.6 and 0.9 equiv) as these merged with the broad signal of piperazine and solvent protons. Downfield shift for the triazolyl and methylene protons may arise due to complexation of the Hg^{2+} through triazolyl nitrogen as it is expected to withdraw electron density from the triazole-piperazine core and to some extent from the vicinal methylene protons^{14b} Moreover, Hg^{2+} -probe interaction is achieved by the orientation changes^{14c} in the probe, which may also contribute to the shift in proton probe signals.

Characteristic vibrations due to NO_3^- at 1384 cm^{-1} in the IR spectrum of $7 \cdot Hg^{2+}$ indicated its presence in the ensuing species (Fig. S16, ESI[†]). Formation of $7 \cdot Hg^{2+}$ has further been supported by HRMS studies. In its HRMS, $7 \cdot Hg^{2+}$ displayed a peak associated with $[M + H]^+$ at 1231.3483 ($7 + Hg^{2+} + 2NO_3^- + 2H_2O$) and 1174.3593 ($7 + Hg^{2+} + NO_3^- + CH_3CN$) and ardently evidenced formation of the aforesaid species (Figs. S14–S15, ESI[†]).

Major Hg^{2+} probes are known to exhibit ‘turn off’ response¹⁵ due to Hg^{2+} induced spin-orbit coupling, in turn, CHEQ (chelation-enhanced quenching).^{3a} Our probe exhibited remarkable fluorescence quenching which may be attributed to the complexation of **7** with Hg^{2+} through piperazine and triazole nitrogens,^{15,13c} consequently, reducing electron density on the fluorophore (BODIPY), leading to oxidative photoinduced electron transfer (PET) (Fig. S24, ESI[†]).

To account for rather inert behavior of **4–6** toward various metal ions and to have better understanding of binding mode and optical response of **7** toward Hg^{2+} energy optimization and frequency calculations have been performed on **4–7** and $7 \cdot Hg^{2+}$. Optimized structures clearly exhibited that piperazine unit adopted chair form in **4–6** in contrary to the twisted boat form in **7** (Fig. 6). This twisted boat form of piperazine unit in **7** clearly accounted for binding of this molecule to the metal ion. Two triazole units in **7** created by double click reaction forces the piperazine nitrogen to come closer, thereby facilitate interaction of the metal ion with donor atoms. After Hg^{2+} coordination, two previously diagonally placed triazole units in **7** become facial and facilitate complexation. Hg^{2+} binds to **7** through two nitrogens one each from piperazine (3.88, 3.96 Å) and triazole units (4.02, 3.87 Å).¹⁶

In many BODIPY-based probes, incorporation of a chelator at *meso*-position of the BODIPY fluorophore decouples two subunits owing to almost perpendicular arrangement of fluorophore and chelator.^{6c} In our case too, optimized structure revealed perpendicular arrangement of the

BODIPY unit and piperazine-triazazole chelator. It also supported oxidative-PET induced quenching upon interaction with Hg^{2+} ion.

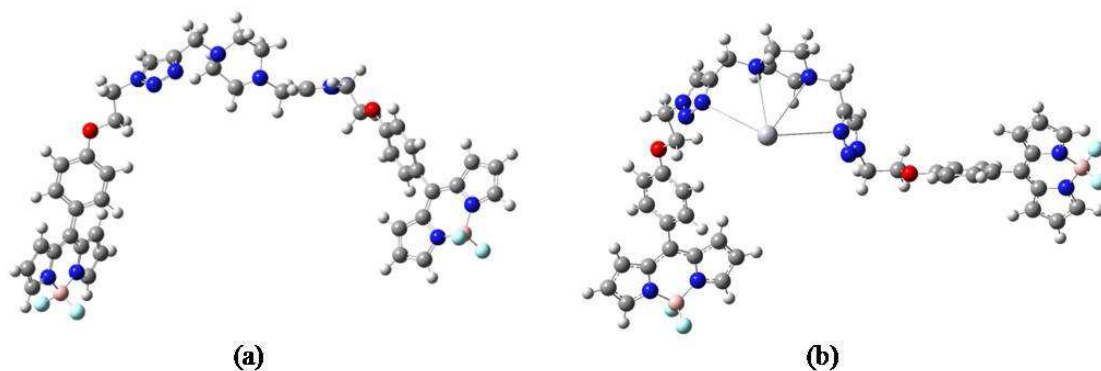


Fig. 6 (a) DFT-optimized structure of **7** (b) **7**· Hg^{2+} complexes.

Conclusion

In summary, through this work we have described piperazine conjugates embracing BODIPY as fluorophore and piperazine along with triazole unit as chelator, separated by alkyl spacers. The compounds **4**, **5**, **6** and **7** have been synthesized by click reactions between azido BODIPY and alkynes imparting substituted and unsubstituted piperazine. Amongst these **7** displays selective response toward Hg^{2+} by oxidative PET, which has been supported by various studies, particularly optical (UV-vis, Fluorescence), HRMS and ^1H NMR titration.

Experimental Section

Reagents. . The solvents were dried and distilled prior to their use following standard literature procedures.¹⁷ Pyrrole, trifluoroacetic acid, 4-hydroxybenzaldehyde, propargyl bromide, piperazine, 1-methylpiperazine, 1-ethylpiperazine, 1-(2-pyridyl)piperazine, 2,3-dichloro-5,6-dicyano-1,4-benzoquinone (DDQ), triethylamine and boron trifluoride diethyl etherate were procured from Sigma Aldrich India and used as received without further purifications. Metal nitrates *viz.*, NaNO_3 , KNO_3 , $\text{Ca}(\text{NO}_3)_2 \cdot 4\text{H}_2\text{O}$, $\text{Mg}(\text{NO}_3)_2 \cdot 6\text{H}_2\text{O}$, FeCl_3 , $\text{Co}(\text{NO}_3)_2 \cdot 6\text{H}_2\text{O}$, $\text{Ni}(\text{NO}_3)_2 \cdot 6\text{H}_2\text{O}$, $\text{Cu}(\text{NO}_3)_2 \cdot 3\text{H}_2\text{O}$, $\text{Zn}(\text{NO}_3)_2 \cdot 6\text{H}_2\text{O}$, $\text{Cd}(\text{NO}_3)_2 \cdot 4\text{H}_2\text{O}$, AgNO_3 , $\text{Pb}(\text{NO}_3)_2$, $\text{Hg}(\text{NO}_3)_2$, $\text{Cr}(\text{NO}_3)_3 \cdot 9\text{H}_2\text{O}$ were obtained from *s.d. fine chem* India Pvt. Ltd and used without further purifications. The azido BODIPY **2** was synthesized following literature procedure.¹⁸

Alkynes **3a–3d** were synthesized by conventional propargylation reactions using propargyl bromide and K_2CO_3 .

Synthesis of 4: Azide functionalized BODIPY **2** (0.353 g, 1 mmol) and alkyne **3a** (0.138g, 1 mmol) were dissolved in THF/ H_2O (1:1) in a round bottom flask and $CuSO_4 \cdot 5H_2O$ (0.012 g, 0.05 mmol per propargyl group) and sodium L-ascorbate (0.02 g, 0.1 mmol per propargyl group) were added with stirring. The reaction mixture was allowed to stir at room temperature for 24h. After completion of the reaction (ensured by TLC) DCM was added to the reaction mixture and washed with saturated aqueous NH_4Cl (2×10 mL), water (10 mL) and brine (10 mL). The organic layer was separated and dried over Na_2SO_4 and concentrated to dryness to afford the crude product. It was purified by flash chromatography and desired product isolated as bright orange solid. Yield: 0.428 g, 88% Analytical data: Anal. Calc. for $C_{25}H_{28}BF_2N_7O$: C, 61.11; H, 5.74; N, 19.95. Found: C, 61.05; H, 5.53; N, 19.54%. 1H NMR ($CDCl_3$, δ ppm): 2.60 (3H, s, methyl-H), 2.89 (8H, m, piperazine-H), 3.82 (2H, s, methylene), 4.47 (2H, s, methylene-H), 4.82 (2H, s, methylene-H), 6.47 (2H, s, pyrrolic-H), 6.93 (2H, s, pyrrolic-H), 7.02 (2H, d, $J = 8.4$ Hz, aromatic-H), 7.50 (2H, m, aromatic-H), 7.79 (1H, s, triazolyl-H), 7.91 (2H, s, pyrrolic-H). ^{13}C NMR ($CDCl_3$, δ ppm): 49.6, 52.4, 52.9, 66.6, 114.5, 118.5, 124.1, 127.2, 131.3, 132.4, 134.8, 143.7, 146.8, 160.2. ^{11}B NMR ($CDCl_3$, δ ppm): 0.25 (t, J (B,F) = 28.8 Hz). ^{19}F NMR ($CDCl_3$, δ ppm): -145. IR (KBr pellet, cm^{-1}): 2926, 1603, 1575, 1544, 1413, 1387, 1261, 1117. UV-Vis. (λ_{max} nm, ϵ $M^{-1} cm^{-1}$): 386 (8×10^3), 474 (1.4×10^4), 494 (3.2×10^4).

Synthesis of 5: It was prepared following the above procedure for **4** using **3b** (0.152 g, 1 mmol) in place of **3a**. Yield: 0.462 g, 91% Analytical data: Anal. Calc. for $C_{26}H_{30}BF_2N_7O$: C, 61.79; H, 5.98; N, 19.40. Found: C, 61.51; H, 5.64; N, 19.11%. 1H NMR ($CDCl_3$, δ ppm): 1.31 (3H, t, methyl-H), 2.90 (10H, br, piperazine-H and methylene proton), 3.82 (2H, s, methylene-H), 4.48 (2H, t, methylene-H), 4.83 (2H, d, methylene-H), 6.55 (2H, s, pyrrolic-H), 6.93 (2H, s, pyrrolic-H), 7.03 (2H, d, $J = 8.7$ Hz, aromatic-H), 7.54 (2H, d, $J = 8.4$ Hz, aromatic-H), 7.78 (1H, s, triazolyl-H), 7.92 (2H, s, pyrrolic-H); ^{13}C NMR ($CDCl_3$, δ ppm): 49.7, 51.3, 52.0, 52.2, 66.5, 114.6, 118.5, 127.2, 131.3, 132.5, 134.8, 143.7, 146.8, 160.1. ^{11}B NMR ($CDCl_3$, δ ppm): 0.25 (t, J (B,F) = 28.8 Hz). ^{19}F NMR ($CDCl_3$, δ ppm): -145. IR (KBr pellet, cm^{-1}): 2925, 1603, 1575, 1544, 1412, 1387, 1260, 1117, 1078. UV-Vis. (λ_{max} nm, ϵ $M^{-1} cm^{-1}$): 385 (8.9×10^3), 473 (1.5×10^4), 495 (3.4×10^4).

Synthesis of 6: It was prepared following the above procedure for **4** using **3c** (0.201 g, 1 mmol) in place of **3a**. Yield: 0.440 g, 78% Analytical data: Anal. Calc. for $C_{29}H_{29}BF_2N_8O$: C, 62.83; H, 5.27; N, 20.21. Found: C, 62.59; H, 5.14; N, 20.08%. 1H NMR ($CDCl_3$, δ ppm): 2.67 (4H, m, piperazine-H), 3.57 (4H, m, piperazine-H), 3.76 (2H, s, methylene-H), 4.48 (2H, t, methylene-H), 4.82 (2H, d, $J = 4.5$ Hz, methylene-H), 6.60 (3H, m, 2 pyrrolic-H and 1 pyridyl-H), 6.97 (4H, dd, 2 pyrrolic-H and 2 aromatic-H), 7.49 (3H, m, 2 aromatic-H and 1 pyridyl-H), 7.75 (1H, s, triazolyl-H), 7.92 (2H, s, pyrrolic-H), 8.17 (2H, t, pyridyl-H). ^{11}B NMR ($CDCl_3$, δ ppm): 0.25 (t, J (B,F) = 28.8 Hz). ^{19}F NMR ($CDCl_3$, δ ppm): -145. IR (KBr pellet, cm^{-1}): 2925, 1668, 1594, 1544, 1480, 1436, 1387, 1247, 1117. UV-Vis. (λ_{max} nm, ϵ $M^{-1} cm^{-1}$): 386 (9.4×10^3), 472 (1.5×10^4), 496 (3.5×10^4).

Synthesis of 7: This compound was prepared following the above procedure for **4** using **3d** (0.162 g, 1 mmol) in place of **3a**. The alkyne and azide were taken in 1:2 ratio. Yield: 0.701 g, 80%. Analytical data: Anal. Calc. for $C_{44}H_{42}B_2F_4N_{12}O_2$: C, 60.85; H, 4.87; N, 19.35. Found: C, 60.69; H, 4.72; N, 19.14% 1H NMR ($CDCl_3$, δ ppm): 2.60 (8H, m, piperazine-H), 3.71 (2H, d, $J = 7.2$ Hz, methylene-H), 4.45 (2H, s, methylene-H), 4.79 (2H, s, methylene-H), 6.55 (2H, s, pyrrolic-H), 6.92 (2H, s, pyrrolic-H), 6.99 (2H, d, $J = 8.4$ Hz, aromatic-H), 7.51 (2H, d, $J = 8.4$ Hz, aromatic-H), 7.69 (1H, s, triazolyl-H), 7.92 (2H, s, pyrrolic-H). ^{13}C NMR ($CDCl_3$, δ ppm): 49.6, 52.4, 52.9, 66.5, 109.4, 114.5, 118.5, 127.2, 131.3, 132.4, 134.7, 143.7, 146.8, 160.1. ^{11}B NMR ($CDCl_3$, δ ppm): 0.25 (t, J (B,F) = 28.8 Hz); ^{19}F NMR ($CDCl_3$, δ ppm): -145. IR (KBr pellet, cm^{-1}): 2933, 1603, 1875, 1545, 1413, 1388, 1261, 1118. UV-Vis. (λ_{max} nm, ϵ $M^{-1} cm^{-1}$): 350 (2.1×10^4), 470 (1.7×10^4), 493 (3.2×10^4).

Theoretical studies. Quantum chemical calculations were performed at the B3LYP Density Functional Theory (DFT) level using B3LYP/6-31G** for **4–7** and B3LYP/LANL2DZ for **7·Hg²⁺** complex.¹⁹ All the geometry optimizations and frequency calculations (to verify a genuine minimum energy structure) were performed using Gaussian 09 suits of program.²⁰

Acknowledgments

Financial support from the Department of Science and Technology (DST), New Delhi through the Scheme SR/S1/IC-25/2011 is gratefully acknowledged. RSS acknowledges the University Grants Commission, New Delhi, India for a Senior Research Fellowship (19-12/2010(i)EU-IV). We also thank the Head Department of Chemistry, Faculty of Science, Banaras Hindu University, Varanasi, India for extending laboratory facilities.

References and notes

- 1 (a) E. Merian, M. Anke, M. Ihnat, M. Stoepler, (eds) Elements and their Compounds in the Environment Occurrence, Analysis and Biological Relevance 2nd edn, Vol. 2 (Wiley, 2004); (b) Y. Zhuang, J. S. Thompson, C. J. Zygarlicke, J. Pavlish, *Environ. Sci. Technol.* 2004, **38**, 5803–5808; (c) Z. Xu, S. J. Han, C. Lee, J. Yoon, D. R. Spring, *Chem. Commun.* 2010, **46**, 1679–1681; (d) A. K. Mandal, M. Suresh, E. Suresh, S. K. Mishra, S. Mishra, A. Das, *Sensors and Actuators B*, 2010, **145**, 32–38.
- 2 (a) P. B. Tchounwou, W. K. Ayensu, N. Ninashvili, D. Sutton, *Environ. Toxicol.* 2003, **18**, 149; (b) D. P. Wojcik, M. E. Godfrey, D. Christie, B. E. Haley, *Neuroendocrinol. Lett.*, 2006, **27**, 415–423.
- 3 (a) D. S. McClure, *J. Chem. Phys.*, 1952, **20**, 682–686; (b) S. Saha, P. Mahato, M. Baidya, S. K. Ghosh, A. Das, *Chem. Commun.*, 2012, **48**, 9293–9295.
- 4 (a) X. Ma, J. Wang, Q. Shan, Z. Tan, G. Wei, D. Wei, Y. Du, *Org. Lett.*, 2012, **14**, 820–823; (b) J. Hu, T. Wu, G. Zhang, S. Liu, *Macromolecules*, 2012, **45**, 3939–3947; (c) Ce'sar Díez-Gil, R. Martí'nez, I. Ratera, T. Hirsh, A. Espinosa, A. Ta'rraga, P. Molina, O. S. Wolfbeisd and J. Veciana, *Chem. Commun.*, 2011, **47**, 1842–1844; (d) L. Zhang, H. Chang, A. Hirata, H. Wu, Q. K. Xue, M. Chen *acs nano*, 2013, **7**, 4595–4600; (e) S. Mukhopadhyay, A. Biswas, R. Pandey, R. K. Gupta, D. S. Pandey, *Tetrahedron Letters*, 2014, **55**, 1437–1440.
- 5 (a) C. Wang, K. M.-C. Wong, *Inorg. Chem.*, 2013, **52**, 13432–13441; (b) C. Liu, S. Huang, H. Yao, S. He, Y. Lu, L. Zhaoab, X. Zeng, *RSC Adv.*, 2014, **4**, 16109–16114; (c) C. Y. Li, X. B. Zhang, L. Qiao, Y. Zhao, C. M. He, S. Y. Huan, L. M. Lu, L. X. Jian, G. L. Shen, R. Q. Yu, *Anal. Chem.*, 2009, **81**, 9993–10001; (d) Y. Ikawa, M. Takeda, M. Suzuki, A. Osuka, H. Furuta, *Chem. Commun.*, 2010, **46**, 5689–5691; (e) X. Zhang, X. Jing, T. Liu, G. Han, H. Li, C. Duan, *Inorg. Chem.*, 2012, **51**, 2325–2331.
- 6 (a) A. Loudet, K. Burgess, *Chem Rev*, 2007, **107**, 4891–4932; (b) S. Suzuki, M. Kozaki, K. Nozaki, K. Okada, *J Photochem Photobiol C Photochem Rev*, 2011, **12**, 269–292; (c) N. Boens, V. Leen, W. Dehaen, *Chem Soc Rev*, 2012, **41**, 1130–1172; (d) Y. Cakmak, E. U. Akkaya, *Org. Lett.* 2009, **11**, 85–88. (e) A. Bozdemir, R. Guliyev, O. Buyukcakir, S. Selcuk, S. Kolemen, G. Gulseren, T. Nalbantoglu, H. Boyaci, E. U. Akkaya, *J. Am. Chem. Soc.* 2010, **132**, 8029–8036; (f) Swamy P, C. A.; Mukherjee, S.; Thilagar, P. *Chem. Commun.*, **2013**, *49*, 993–995.

- 7 (a) Y. H. Lau, P. J. Rutledge, M. Watkinson, M. H. Todd, *Chem. Soc. Rev.*, 2011, **40**, 2848–2866; (b) Q. Y. Cao, Y. M. Han, H. M. Wang, Y. Xie, *Dyes and Pigments*, 2013, **99**, 798–802; (c) X. Zhang, Y. Xiao, J. Qi, J. Qu, B. Kim, X. Yue, K. D. Belfield, *J. Org. Chem.*, **2013**, **78**, 9153–9160; (d) C. Dragonetti, A. Valore, A. Colombo, S. Righetto, V. Trifiletti, *Inorganica Chimica Acta*, 2012, **388**, 163–167. (e) P. K. Muwal, S. Pandeya, P. S. Pandey, *RSC Adv.*, 2014, **4**, 21531–21534. (f) A. Thakur, D. Mandal, P. Deb, B. Mondal, S. Ghosh, *RSC Adv.*, 2014, **4**, 1918–1928.
- 8 M. Nolte, I. Pantenburg, G. Meyer, *Z. Anorg. Allg. Chem.* 2005, **631**, 2923–2927.
- 9 C. Zhang, J. Zhao, S. Wu, Z. Wang, W. Wu, J. Ma, S. Guo, L. Huang, *J Am Chem Soc.*, 2013, **135**, 10566–10578.
- 10 V. Lakshmi, M. Ravikanth, *Dalton Trans.*, 2012, **41**, 5903–5911.
- 11 (a) R. S. Singh, M. Yadav, R. K. Gupta, R. Pandey, D. S. Pandey, *Dalton Trans.*, 2013, **42**, 1696–1707; (b) S. J. Smalley, M. R. Waterland, S. G. Telfer, *Inorg. Chem.*, 2009, **48**, 13–15; (c) K. Hanson, A. Tamayo, V. V. Diev, M. T. Whited, P. I. Djurovich, M. E. Thompson, *Inorg. Chem.*, 2010, **49**, 6077–6084; (d) T. Lazarides, T. M. McCormick, K. C. Wilson, S. Lee, D. W. McCamant, R. Eisenberg, *J. Am. Chem. Soc.*, 2011, **133**, 350–364.
- 12 S. Goswami, A. K. Das, S. Maity, *Dalton Trans.*, 2013, **42**, 16259–16263.
- 13 (a) S. H. Lee, A. Parthasarathy, K. S. Schanze, *Macromol. Rapid Commun.*, 2013, **34**, 791–795; (b) F. Miao, J. Zhan, Z. Zou, D. Tian, H. Li, *Tetrahedron*, 2012, **68**, 2409–2413; (c) H. F. Wang, S. P. Wu, *Tetrahedron*, 2013, **69**, 1965–1969.
- 14 (a) M. Kaupp, O. L. Malkina, V. G. Malkin, P. Pyykko, *Chem. Eur. J.*, 1998, **4**, 118–126; (b) E. Manandhar, J. H. Broome, J. Myrick, W. Lagrone, P. J. Cragg, K. J. Wallace, *Chem. Commun.*, 2011, **47**, 8796–8798; (c) A. Singh, S. Kaur, N. Singh, N. Kaur, *Org. Biomol. Chem.*, 2014, **12**, 2302–2309.
- 15 (a) K. Ghosh, D. Tarafdar, A. Samadderb, A. R. Khuda-Bukhsh, *New J. Chem.*, 2013, **37**, 4206–4213; (b) G. Angelovski, B. Costisella, B. Kolaric', M. Engelhard, P. Eilbrachtartin, *J. Org. Chem.* 2004, **69**, 5290–5294; (c) N. J. Wang, C. M. Sun, W. S. Chung, *Tetrahedron*, 2011, **67**, 8131–8139.
- 16 K. H. Chen, C.Y. Lu, H. J. Cheng, S. J. Chen, C. H. Hu, A.T. Wu, *Carbohydrate Research*, 2010, **345**, 2557–2561.

- 17 D. D. Perrin, W. L. F. Armango, D. R. Perrin, *Purification of laboratory Chemicals*, Pergamon: Oxford, U.K. 1986.
- 18 C. Zhang, J. Zhao, S. Wu, Z. Wang, W. Wu, J. Ma, S. Guo, L. Huang, *J Am Chem Soc.*, **2013**, *135*, 10566-10578.
- 19 (a) Y. Zhou, Y. Xiao, D. Li, M. Fu, X. Qian, *J. Org. Chem.*, 2008, **73**, 1571–1574; (b) P. E. Burrows, Z. Shen, V. Bulovic, D. M. McCarty, S. R. Forrest, J. A. Cronin, M. E. Thompson, *J. Appl. Phys.*, 1996, **79**, 7991–8006.
- 20 M. J. Frisch, G. W. Trucks, H. B. Schlegel, G. E. Scuseria, M. A. Robb, J. R. Cheeseman, G. Scalmani, V. Barone, B. Mennucci, G. A. Petersson, H. Nakatsuji, M. Caricato, X. Li, H. P. Hratchian, A. F. Izmaylov, J. Bloino, G. Zheng, J. L. Sonnenberg, M. Hada, M. Ehara, K. Toyota, R. Fukuda, J. Hasegawa, M. Ishida, T. Nakajima, Y. Honda, O. Kitao, H. Nakai, T. Vreven, J. A. Montgomery, Jr., J. E. Peralta, F. Ogliaro, M. Bearpark, J. J. Heyd, E. Brothers, K. N. Kudin, V. N. Staroverov, R. Kobayashi, J. Normand, K. Raghavachari, A. Rendell, J. C. Burant, S. S. Iyengar, J. Tomasi, M. Cossi, N. Rega, J. M. Millam, M. Klene, J. E. Knox, J. B. Cross, V. Bakken, C. Adamo, J. Jaramillo, R. Gomperts, R. E. Stratmann, O. Yazyev, A. J. Austin, R. Cammi, C. Pomelli, J. W. Ochterski, R. L. Martin, K. Morokuma, V. G. Zakrzewski, G. A. Voth, P. Salvador, J. J. Dannenberg, S. Dapprich, A. D. Daniels, Ö. Farkas, J. B. Foresman, J. V. Ortiz, J. Cioslowski, and D. J. Fox, *Gaussian 09, revision A.1*, Gaussian, Inc., Wallingford, CT, 2009.